applied sciences

MDPI

Article

Studies on the Synthesis and Application Properties of a Betaine Surfactant with a Benzene Ring Structure

Qi Zuo [1,2,3], Zhihui Wang [1,2,3], Peng Li [3], Luyuan Yang [3] and Zhaozheng Song [3,*]

[1] State Key Laboratory of Shale Oil and Gas Enrichment Mechanisms and Effective Development, Beijing 102206, China
[2] Research and Development Center for the Sustainable Development of Continental Sandstone Mature Oilfield by National Energy Administration, Beijing 102206, China
[3] College of Science, China University of Petroleum, Beijing 102249, China
* Correspondence: song@cup.edu.cn

Abstract: Two novel betaine surfactants with distinct hydrophilic headgroups were synthesized, including carboxybetaine surfactant (DCB) and sulfobetaine surfactant (DSB). Their properties of reducing the interfacial tension (IFT) of Xinjiang crude oil/water were studied under alkaline-free conditions, as were their thermal stability, wettability, and emulsification properties. The chemical structures of the target products were characterized and analyzed by using ^{1}H-NMR and ^{13}C-NMR. The experimental results indicate that the introduction of a benzene ring to the hydrophobic group can improve the solubility and high-temperature resistance of the betaine surfactant. Thermogravimetric analysis showed that the degradation temperature of the synthesized betaine was above 190 °C. As the concentration of the betaine solution increased, DSB (0.0750 mmol/L) showed a lower critical micelle concentration (CMC) than DCB (0.1852 mmol/L). The wetting ability of DCB was significantly higher than that of DSB, and their contact angles on paraffin film decreased to 28.36° and 35.26°. In addition, both DCB and DSB can reduce the IFT of Xinjiang crude oil/water to ultra-low levels (10^{-3} mN/m) in the absence of alkali. The appropriate ion concentration has a synergistic effect on the surfactant to reduce the interfacial tension of oil/water and the effect of the three ions on the interfacial tension was as follows: $Na^{+} < Ca^{2+} < Mg^{2+}$.

Keywords: betaine surfactant; temperature resistance; interfacial tension; critical micelle concentration

Citation: Zuo, Q.; Wang, Z.; Li, P.; Yang, L.; Song, Z. Studies on the Synthesis and Application Properties of a Betaine Surfactant with a Benzene Ring Structure. *Appl. Sci.* **2023**, *13*, 4378. https://doi.org/10.3390/app13074378

Academic Editor: Maria Annunziata M. Capozzi

Received: 7 February 2023
Revised: 27 March 2023
Accepted: 28 March 2023
Published: 30 March 2023

1. Introduction

With the increasing consumption of oil, ordinary reservoirs have been unable to meet demand; so high-temperature and high-salt reservoirs have become important for oil exploitation in the future. There are both positive and negative charge centers in the hydrophilic groups of zwitterionic surfactants, which are electrically neutral, so, compared with other types of ionic surfactants, the charge repulsion force will be weakened, and the arrangement on the interface is more compact and has a better interface performance [1–4]. Betaine surfactants are typical zwitterionic surfactants. Due to their excellent biodegradability, high temperature and salt resistance, and good compound performance, betaine surfactants have attracted much attention from researchers in recent years [5,6]. A betaine molecule always exists in the form of an internal salt, so it can adapt to the environment of strong acid or strong alkali without becoming sensitive to the change of pH in solution [7]. At the same time, this structure is less affected by electrolytes and has better stability in high salinity, so it is widely used as an oil displacement agent in tertiary oil recovery [8,9].

As one of the best potential technologies of EOR, the addition of alkali has caused many adverse effects, such as formation damage, equipment corrosion, a shortened pump inspection cycle, and difficult demulsification of produced fluid [10–13]. Therefore, there is an urgent need to develop an alkali-free surfactant for oil flooding. As we all know, an important factor determining the properties of betaine surfactants is their chemical

structure. In recent years, many studies have been carried out on the effect of modifying hydrophobic groups, hydrocarbon chain length, and the types of hydrophilic headgroup. For example, according to the similar compatibility principle, benzene rings inserted into hydrophobic groups will strongly interact with aromatic hydrocarbon components in crude oil, exhibiting a lower critical micelle concentration (CMC), ultra-low interfacial tension (IFT), and excellent wettability alteration [14–16]. Sulfobetaine surfactants exhibit better salt tolerance and are more efficient in alkali-free oil flooding, and carboxybetaine surfactants showed better surface properties [17–20].

In this study, two kinds of new and high-performance betaine surfactants with a benzene ring structure and different hydrophilic groups were synthesized: 1-((3-(4-dodecylphenoxy)-2-hydroxypropyl)dimethylammonio)acetate and 2-((3-(4-dodecylphenoxy)-2-hydroxypropyl)dimethylammonio)-2-hydroxypropane-1-sulfonate. This paper aims to research and develop a surfactant for oil flooding without alkali, with excellent properties of high temperature resistance and salt resistance. The chemical structures of the target products were characterized and analyzed using ^{1}H-NMR and ^{13}C-NMR. The physicochemical properties of DCB and DSB were evaluated using thermogravimetric analysis and surface tension measurement. The wettability, emulsification performance, and interfacial tension of the two betaine surfactant solutions were systematically studied to evaluate their application in enhanced oil recovery.

2. Materials and Methods

2.1. Materials

4-Dodecylphenol (98%), epichlorohydrin (ECH) (99%), and dimethylamine solution (40%) were purchased from Macklin Co. (Shanghai, China). Tetrabutyl ammonium bromide (TBAB) (99%), *N*,*N*-dimethylglycine (98%), and sodium 3-chloro-2-hydroxypropane-1-sulfonate (98%) were purchased from Aladdin Co. (Shanghai, China). Sodium bicarbonate (99%), anhydrous sodium sulfate (98%), and sodium chloride (99%) were obtained from Tianjin Guangfu Co. (Tianjin, China). All organic solvents, including dichloroethane, ethyl acetate, petroleum ether, methanol, ethanol, and acetone, were of analytical grade and supplied by Tianjin Fuyu Chemical Works (Tianjin, China).

2.2. Synthesis and Characterization

The two kinds of new phenyl-containing surfactants were synthesized following the pathway in Scheme 1. The NMR spectra were obtained on a BRUKER AVANCE III (Bruker, Billerica, MA, USA) in $CDCl_3$ (δ 7.26 and δ 77.3) and CD_3OD (δ 3.31 and δ 49.7), operated at 500 MHz. The ^{1}H NMR and ^{13}C NMR spectra of products are shown in the Supplementary Materials (Figures S1–S6).

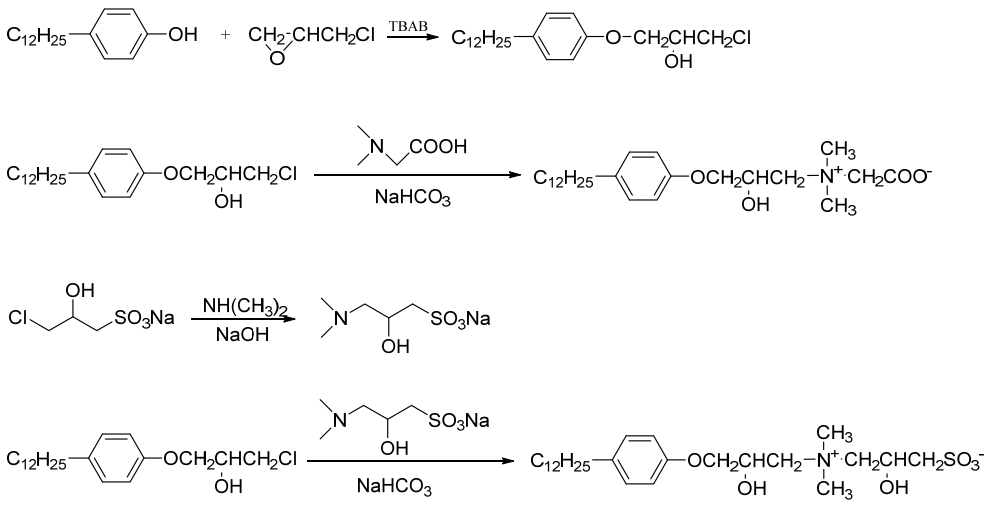

Scheme 1. Synthesis of DCB and DSB.

2.2.1. Synthesis of 1-Chloro-3-(4-dodecylphenoxy)propan-2-ol

Tetrabbutylammonium bromide (0.002 mol, 0.65 g) was added as a catalyst to a 100-mL three-mouth flask containing dodecyl phenol (0.05 mol, 13.12 g) and epichlorohydrin (0.2 mol, 18.5 g). The mixture was reacted at 85 °C for 1.5 h and then the temperature was increased to 95 °C for 3.5 h. After the reaction, the excess epxychlorohydrin was evaporated under reduced pressure (−0.08 MPa/65°C). The product was purified using column chromatography and eluted with petroleum ether and ethyl acetate (20:1).

1-Chloro-3-(4-dodecylphenoxy)propan-2-ol: Colorless liquid, yield (76%), **^{1}H NMR** (500 MHz, $CDCl_3$) δ 0.88–0.90 (t, 3H, Ar–CH_2–CH_2–CH_2–$(CH_2)_8$–***CH_3***), 1.24–1.28 (m, 16H, Ar–CH_2–CH_2–CH_2–***$(CH_2)_8$***–CH_3), 1.34–1.37 (m, 2H, Ar–CH_2–CH_2–***CH_2***–$(CH_2)_8$–CH_3), 1.52–1.61 (m, 2H, Ar–CH_2–***CH_2***–CH_2–$(CH_2)_8$–CH_3), 2.53–2.54 (d, 1H,Ar–O–CH_2–CH(***OH***)–CH_2–Cl), 2.53–2.64 (m, 2H,Ar–***CH_2***–CH_2–CH_2–$(CH_2)_8$–CH_3), 3.66–3.71 (m, 2H, Ar–O–CH_2–CH(OH)–***CH_2***–Cl), 3.75–3.77, 4.19–4.20 (m, 2H, Ar–O–***CH_2***–CH(OH)–CH_2–Cl), 4.05–4.07 (m, 1H, Ar–O–CH_2–***CH***(OH)–CH_2–Cl), 6.34 (d, 2H, 1,5–Ar***H***), 7.17–7.19 (d, 2H, 2,4–Ar***H***). ^{13}C NMR (125 MHz, $CDCl_3$) δ 14.13, 22.80, 29.11, 29.35, 29.55, 29.67, 31.52, 35.00, 46.00, 68.50, 70.01, 113.80, 127.24, 140.96, 155.77.

2.2.2. Synthesis of 2-((3-(4-Dodecylphenoxy)-2-hydroxypropyl)dimethylammonio)acetate

Sodium bicarbonate (0.012 mol, 1.01 g) was slowly added to 30 mL ethanol solution with *N*,*N*-dimethylglycine (0.012 mol, 1.24 g) and reacted at 80 °C for 1 h. Then, dodecyl phenol chlorol ether (0.01 mol, 3.54 g) was dissolved in hexane (15 mL) and slowly dropped into the above solution and reacted for 8 h. All solvents were vaporized under reduced pressure (−0.08 MPa/45 °C) to obtain a light yellow waxy viscous betaine crude product. Ethyl acetate (30 mL) was added to the crude product and stirred to reflux for 2 h, then cooled and filtered. The extracted solids were recrystallized several times in methanol and acetone mixed solvent system, and the resulting products were dried under a vacuum at 60 °C for 24 h.

1-((3-(4-Dodecylphenoxy)-2-hydroxypropyl)dimethylammonio)acetate: White solid, yield (79%), **^{1}H NMR** (500 MHz, CD_3OD) δ 0.87–0.90 (t, 3H, Ar–CH_2–CH_2–$(CH_2)_9$–***CH_3***), 1.25–1.37 (m, 18H, Ar–CH_2–CH_2–***$(CH_2)_9$***–CH_3), 1.56–1.62 (m, 2H, Ar–CH_2–***CH_2***–$(CH_2)_9$–CH_3), 2.56–2.58 (d, 1H, Ar–O–CH_2–CH(***OH***)–CH_2–$N^+(CH_3)_2$–CH_2–COO^-), 2.56–2.67 (m, 2H, Ar–***CH_2***–CH_2–CH_2–$(CH_2)_8$–CH_3), 3.13 (s, 6H, Ar–O–CH_2–CH(OH)–CH_2–N^+***$(CH_3)_2$***–CH_2–COO^-), 3.48–3.72 (m, 2H, Ar–O–CH_2–CH(OH)–***CH_2***–$N^+(CH_3)_2$–CH_2–COO^-), 3.93–4.19 (m, 2H, Ar–O–***CH_2***–CH(OH)–CH_2–$N^+(CH_3)_2$–CH_2–COO^-), 4.69–4.74 (m, 1H, Ar–O–CH_2–***CH***(OH)–CH_2–$N^+(CH_3)_2$–CH_2–COO^-), 4.69–5.29 (m, 2H, Ar–O–CH_2–CH(OH)–CH_2–$N^+(CH_3)_2$–***CH_2***–COO^-), 6.82–6.83 (d, 2H, **1,5**–Ar***H***), 7.08–7.09 (d, 2H, **2,4**–Ar**H**). **^{13}C NMR** (125 MHz, CD_3OD) δ 14.12, 22.80, 29.11, 29.35, 29.55, 29.67, 29.79, 31.52, 31.64, 35.00, 52.27, 64.65, 66.10, 66.85, 67,21, 114.96, 128.16, 135.72, 157.47, 169.02.

2.2.3. Synthesis of Sodium 3-(Dimethylamino)-2-hydroxypropane-1-sulfonate

A 40% dimethylamine solution (0.3 mol, 33.83 g) was slowly added to 50 mL deionized water dissolved in sodium 3-chloro-2-hydroxypropanesulfonic acid (0.1 mol, 19.86 g), and sodium hydroxide (0.2 mol, 8.0 g) was added to the mixture. The mixture was stirred at 40 °C for 12 h. A reduction pressure evaporation was used to remove the organic solvent, and hot methanol was used to dissolve the solid. The filtrate evaporated under pressure to get the crude product, which was recrystallized in ethanol many times to get the pure intermediate product.

2.2.4. Synthesis of 3-((3-(4-Dodecylphenoxy)-2-hydroxypropyl)dimethylammonio)-2-hydroxypropane-1-sulfonate

Dodecyl phenol chlorol ether (0.01 mol, 3.54 g) was dissolved into hot ethanol (30 mL), and then sodium 3-(dimethylamino)-2-hydroxypropyl sulfonate (0.012 mol, 2.46 g) and sodium bicarbonate (0.012 mol, 1.01 g) were added to the above stirred solution. The

mixed solution was refluxed for 12 h. The residue was removed by using filtration, and the solvent was vaporized under reduced pressure to obtain the yellowish waxy thick betaine crude product. Ethyl acetate (30 mL) was added to the crude product and stirred to reflux for 2 h, then cooled and filtered. The extracted solids were recrystallized several times in methanol and acetone mixed solvent system, and the resulting products were dried under a vacuum at 60 °C for 24 h.

1-((3-(4-Dodecylphenoxy)-2-hydroxypropyl)dimethylammonio)-2-hydroxypropane-1-sulfonate: White solid, yield (72%), **^{1}H NMR** (500 MHz, CD_3OD) δ 0.87–0.91 (t, 3H, Ar–CH_2–CH_2–$(CH_2)_9$–***CH_3***), 1.21–1.48 (m, 18H, Ar–CH_2–CH_2–***$(CH_2)_9$***–CH_3), 1.61–1.70 (m, 2H, Ar–CH_2–***CH_2***–$(CH_2)_9$–CH_3), 1.96–1.97 (d, 1H, –$N^+(CH_3)_2$–CH_2–CH(***OH***)–$CH_2SO_3^-$), 2.56–2.58 (d, 1H, –CH_2–CH(***OH***)–CH_2–$N^+(CH_3)_2$), 2.51–2.95 (m, 2H, Ar–***CH_2***–CH_2–$(CH_2)_9$–CH_3), 3.19 (s, 6H, –N^+***$(CH_3)_2$***–CH_2–CH(–OH)–$CH_2SO_3^-$), 3.23–3.27, 4.32–4.36 (m, 2H, –$N^+(CH_3)_2$–***CH_2***–CH(–OH)–$CH_2SO_3^-$), 3.40–3.44, 3.91–3.95 (m, 2H, Ar–O–CH_2–CH(OH)–***CH_2***–$N^+(CH_3)_2$), 3.40–3.69, (m, 2H, –$N^+(CH_3)_2$–CH_2–CH(–OH)–***CH_2***–SO_3^-), 3.91–4.30 (m, 2H, Ar–O–***CH_2***–CH(OH)–CH_2–$N^+(CH_3)_2$), 4.61–4.63 (m, 1H, –CH_2–***CH***(OH)–CH_2–$N^+(CH_3)_2$–CH_2–***CH***(–OH)–$CH_2SO_3^-$), 6.84–6.85 (d, 2H, **1,5**–Ar***H***), 7.07–7.08 (d, 2H, **2,4**–Ar***H***). **^{13}C NMR** (125 MHz, CD_3OD) δ 14.13, 22.80, 29.11, 29.35, 29.55,29.67, 29.79, 31.52, 31.64, 35.00, 53.41, 56.33, 63.21, 64.65, 66.09, 66.88, 115.29, 129.10, 135.72, 157.27.

2.3. Measurements

2.3.1. Thermal Stability Measurements

Thermogravimetric analysis (TGA) is a common method to test the thermal stability of surfactants. The instrument used in this experiment was an HTG−3 thermogravimetric analyzer. The argon flow rate was 50 mL·min^{-1} and the heating rate was 10 °C·min^{-1}.

2.3.2. Surface Tension Measurements

The surface tension was measured using the Wilhelmy plate technique on a BZY-2 surface tensiometer. A series of surfactant solutions with gradient concentrations were prepared and placed at room temperature for 24 h to ensure adsorption equilibrium. The surface tension of these solutions was measured at 25 ± 0.2 °C. In order to ensure the accuracy of the experiment, the measurement was repeated three times, and the average value was taken.

2.3.3. Interfacial Tension (IFT) Measurements

The interfacial tension was measured by using a TX-500C rotating droplet interfacial tensiometer. The surfactant solutions with different concentrations and ionic mineralizations were prepared and placed in a 40 ± 0.5 °C constant-temperature water bath for standby use (the formation temperature was set at 40 °C). The rotation speed of the rotating droplet interface tensiometer was 5000 rpm. The viscosity of Xinjiang crude oil was 15.8 mPa·s, and the density was 0.86 g/cm^3.

2.3.4. Wetting Ability

The wetting ability of surfactants is a useful criterion for evaluating its suitability for use in oil recovery and flotation applications [21]. The wettability of the surfactant solution was measured using a JC2000C contact angle meter. The paraffin film was used as the test substrate, 5 μL droplets were injected into the paraffin film using a microsampler, and the change in droplet contact angle was recorded every 2 min for 20 min. Each group of samples was measured three times and averaged. The test was carried out in a confined space and kept at 25 ± 1 °C.

2.3.5. Emulsion Stability

The surfactant solution and crude oil with a volume ratio of 0.6/0.4 in a 100 mL stopper cylinder were violently shaken and placed in a 25 ± 0.5 °C thermostatic water

bath. The time required for the emulsion to separate out 10 mL of water was recorded. The measurements were repeated three times and averaged [22].

3. Results and Discussion

3.1. Thermogravimetric Analysis

The thermal stability of surfactants is usually characterized using thermogravimetric analysis. The thermogravimetric analysis curve Figure 1 showed that the two betaine surfactants did not suffer mass loss at low temperature (<100 °C), indicating that the synthesized product did not undergo phase change at low temperature, and there was no residual solvent. The thermal decomposition temperature of DCB and DSB is 193 °C and 240 °C, and the initial temperature of thermal decomposition of sulfobetaine is much higher than that of carboxyl type. This occurs because the hydroxypropyl sulfonic group is more stable during the heating process and is more suitable for the development of high temperature oil fields [23]. In addition, the introduction of aryl groups changes the bond energy of molecular bonds. C–N and C–C have bond energies of 305 kJ/mol and 347 kJ/mol, respectively, and C–N breaks first during thermal decomposition. However, the benzene ring is an electron-rich structure, which will affect the electron configuration of the nearby chemical bonds and enhance the bond energy of C–N. Therefore, the new arylbetaine surfactants have more potential in high-temperature oil fields than conventional long-chain alkylbetaines.

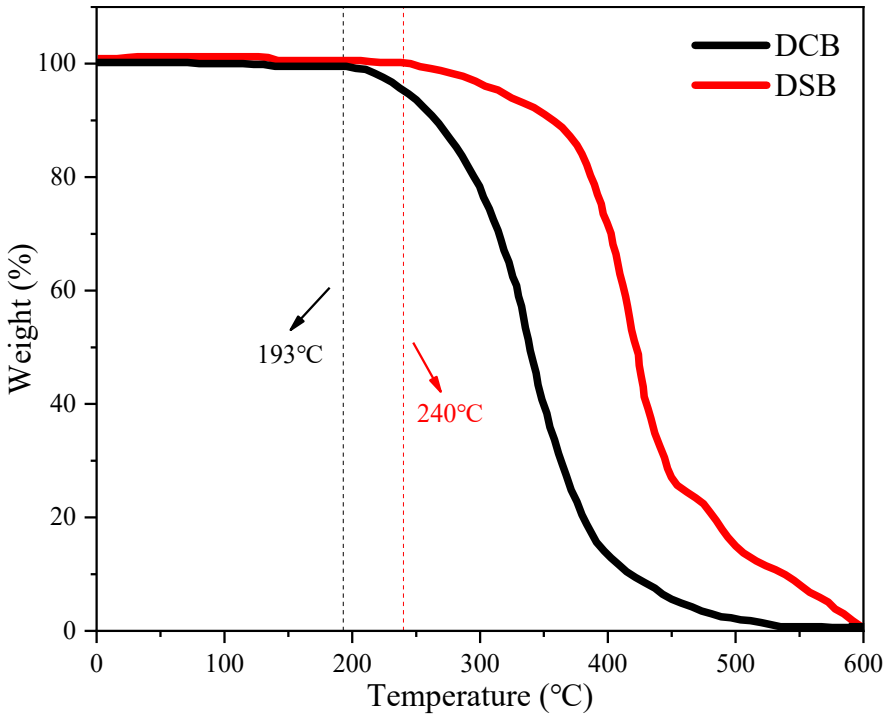

Figure 1. TGA curves of DCB and DSB.

3.2. Equilibrium Surface Tension

The γ-logC curve of betaine surfactants Figure 2 shows that the critical micelle concentration (CMC) value of DCB is 0.1852 mmol/L and that of γ_{CMC} is 27.6 mN/m. The CMC of DSB is 0.0750 mmol/L and that of γ_{CMC} is 30.0 mN/m. When the concentration of the surfactant solution is low, a large number of surfactant molecules adsorb on the surface of the solution, reducing the contact area between water and air, which leads to a sharp drop in surface tension. When the concentration reaches a certain value, the molecules reach saturation adsorption on the surface of the solution, micelles begin to form inside the solution, and the surface tension basically does not change. The concentration corresponding to this point is CMC, and the corresponding surface tension is γ_{CMC}.

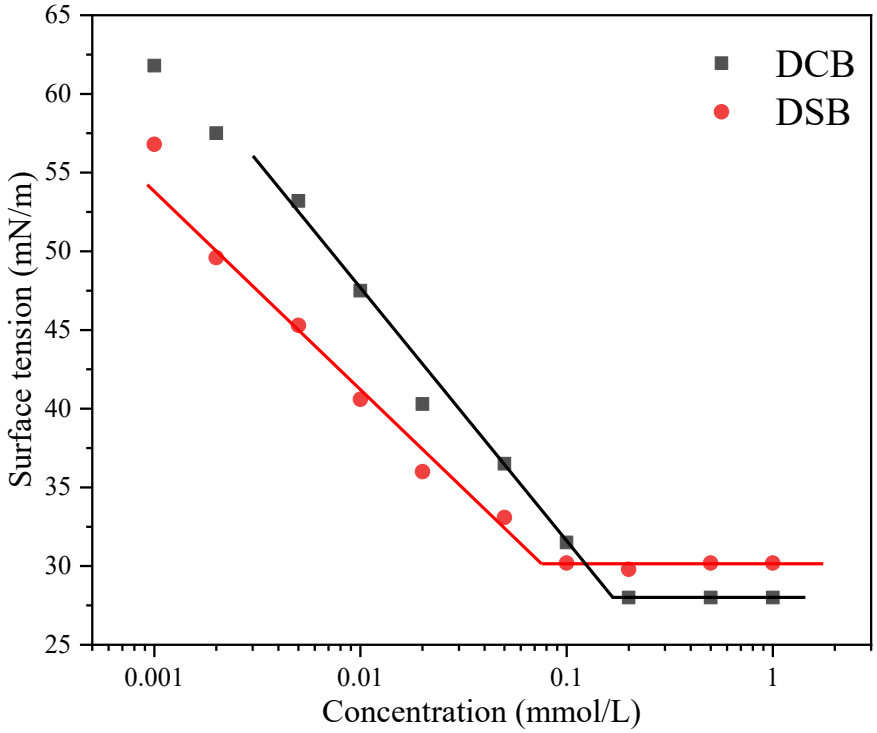

Figure 2. Variation of the surface tension with the surfactant concentration for DCB and DSB at 25 °C.

Both betaine surfactants have the same hydrophobic chain and differ only in the hydrophilic group. On the one hand, the volume of carboxyl group is smaller than that of the hydroxypropyl sulfonic group [24]. With the increase in surfactant concentration, DCB molecules are arranged more closely after saturation and adsorption on the liquid surface. Therefore, the surface tension of DCB is lower than that of DSB. On the other hand, CMC of sulfobetaine is lower than carboxybetaine due to solvation effects [25]. This is because, during micelle formation, the hydroxypropyl sulfonic group and the carboxyl group may have different solvation/desolvation characteristics.

3.3. Interfacial Tension Measurements (IFT)

IFT is an important index of enhanced oil recovery in tertiary oil recovery technology. An excellent surfactant solution is required to form ultra-low interfacial tension (10^{-3} mN/m) with crude oil. At this time, the capillary size of the rock is significantly increased, the starting pressure of residual oil drops is decreased, and the dispersed oil drops gradually gather into oil bands in the pore throat and are displaced. The surfactant solution's interfacial tension with crude oil is usually influenced by its concentration, reservoir temperature, salinity (Na^+, Mg^{2+}, Ca^{2+} plasma concentration), and other factors, and there is a suitable value for the oil–water system to reach the lowest interfacial tension (IFT_{min}).

3.3.1. Effect of Concentration on IFT

The IFT with varying surfactant concentrations is depicted in Figure 3. DCB and DSB can reach ultra-low interface tension with crude oil in the measured concentration range and had better adaptability with Xinjiang crude oil, 3.9×10^{-3} mN/m and 5.5×10^{-3} mN/m, respectively. With the same length of carbon chain, the carboxyl group is more hydrophilic than the hydroxypropyl sulfonic group and exhibits lower IFT at the same solution concentration. Meanwhile, IFT first decreased and then increased with time. When the adsorption and desorption of surfactants at the oil–water interface reached a balance, the interfacial tension approached a certain equilibrium value, which is the dynamic interfacial tension (DIFT) behavior [26,27]. The reason is that there is a dynamic

balance between the adsorption and desorption of surfactant molecules at the oil–water interface, both of which occurred simultaneously. Initially, the adsorption of surfactant molecules at the interface was higher than desorption, and the DIFT decreased as the molecules moved from the inside of the solution to the interface. Then, with the passage of time, the molecules reached adsorption saturation at the interface, the adsorption rate was gradually lower than the desorption rate, and the DIFT increased. Finally, when adsorption and desorption reached equilibrium, DIFT was stable [28].

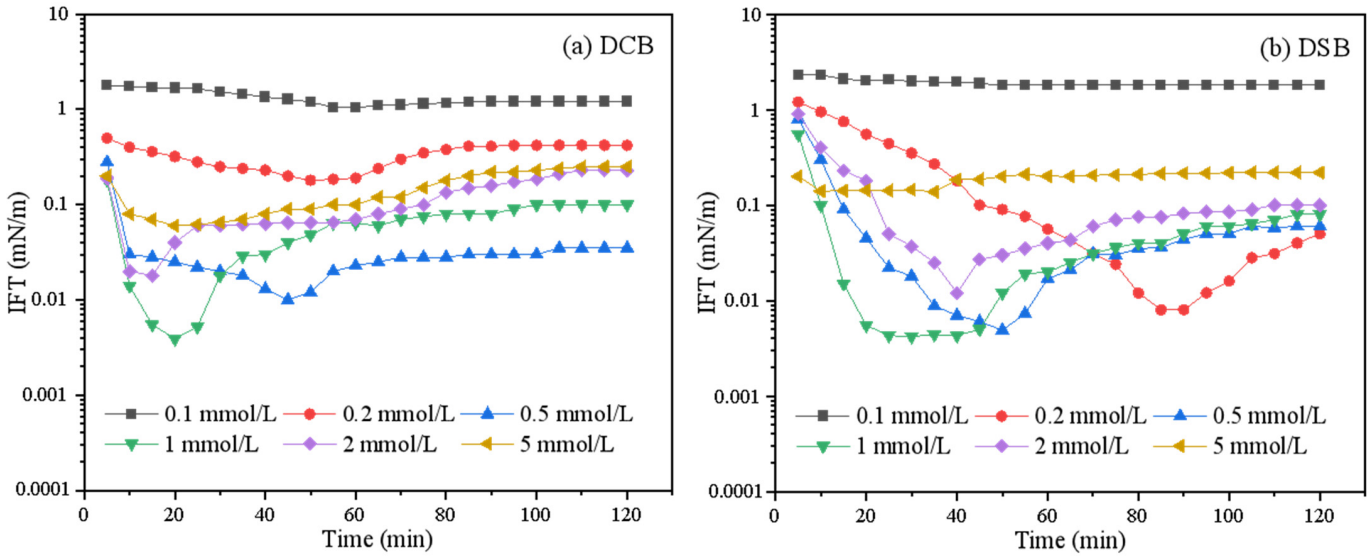

Figure 3. Variation of the interfacial tension with the surfactant concentration for DCB (**a**) and DSB (**b**) against Xinjiang crude oil at 40 °C.

3.3.2. Effect of Temperature on IFT

The effect of temperature on IFT reduction in the surfactant solution was determined. As shown in Figure 4 as the test temperature rose, the time required for the system to the lowest interfacial tension (IFT_{min}) became shorter. According to Brownian motion, with an increase in experimental temperature, the movement speed of the surfactant molecules increases, and the diffusion speed from the solution body to the interface becomes faster, resulting in the IFT reaching the lowest value faster. Furthermore, with an increase in test temperature, IFT_{min} shows a trend of decreasing first and then increasing. On the one hand, an increase in temperature decreases the viscosity of crude oil, which can effectively reduce IFT_{min} [29]. On the other hand, with an increase in the test temperature, the adsorption and desorption rate of molecules on the interface increased, making the interface film more unstable, and the IFT_{min} increased (Table 1).

Table 1. Parameters on the lowest interfacial tension (IFT_{min}) and the equilibrium interfacial tension value (IFT_{equ}) of the required time vary with temperature.

	40 °C	**50 °C**	**60 °C**	**70 °C**
t/min (IFT_{min})	20	15	10	10
DCB (IFT_{min}/mN·m^{-1})	4.0×10^{-3}	2.5×10^{-3}	4.5×10^{-3}	4.3×10^{-2}
DCB (IFT_{equ}/mN·m^{-1})	0.1	0.13	0.4	1.3
t/min (IFT_{min})	35	30	20	15
DSB (IFT_{min}/mN·m^{-1})	3.5×10^{-3}	2.8×10^{-3}	2.7×10^{-3}	1.7×10^{-2}
DSB (IFT_{equ}/mN·m^{-1})	0.075	0.19	0.3	0.51

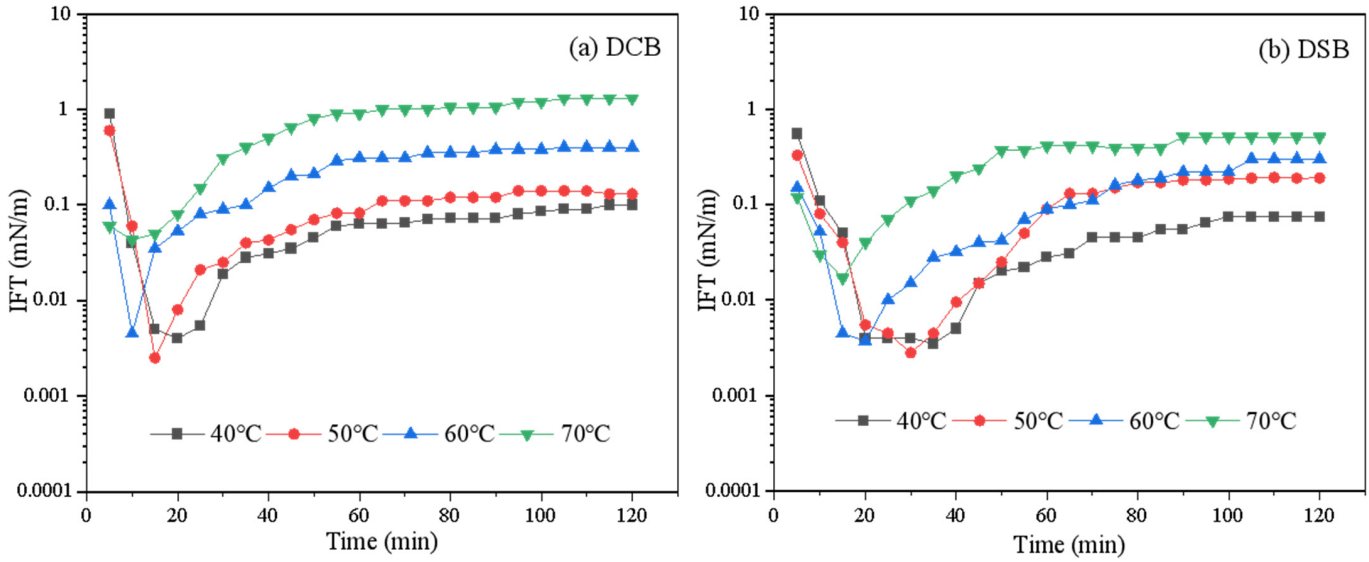

Figure 4. Effects of temperature on IFT between the optimum concentrations of surfactants and Xinjiang crude oil for DCB (**a**) and DSB (**b**).

In addition, the long carbon chain of the surfactant molecule was aggregated with the increase in temperature, and the force with crude oil decreased, resulting in an increase in the equilibrium interfacial tension value (IFT_{equ}) [20].

3.3.3. Effect of NaCl on IFT

The study was conducted to determine the effect of NaCl concentration on the DIFT of betaine surfactant solution at the optimal concentration and Xinjiang crude oil. It was observed that the lowest interfacial tension (IFT_{min}) gradually decreased with the increase in Na^+ concentration and reached the minimum values of 3.0×10^{-4} mN/m and 1.5×10^{-4} mN/m when the Na^+ concentration was 5%. This indicates that NaCl and betaine surfactants have synergistic effects in aqueous solution. Meanwhile, when the concentration of Na^+ reached 10%, DCB and DSB can still reach the state of ultra-low interfacial tension, and both of them had good tolerance to monovalent cations.

It can also be discovered from the Figure 5 that, with an increase in Na^+ concentration, the equilibrium interfacial tension value (IFT_{equ}) of both betaine surfactants showed a trend of first decreasing and then increasing. DCB was lowest (1.9×10^{-2} mN/m) when the Na+ concentration was 2%, and DSB was the lowest (1.5×10^{-3} mN/m) when the Na+ concentration was 5%. The reason is that the surfactant molecules in solution can form a diffusion double electric layer and Na^+ will compress the double electric layer, giving the surfactant molecules in the interface layer a more compact arrangement, leading to a gradual reduction in IFT_{equ} [30]. However, as the concentration of Na^+ continues to increase, the addition of counter ions can shield the charge of the ionic surfactant, destroy the hydration structure around ions, and enhance the hydrophobicity of the surfactant, which leads to the transfer of more surfactant molecules to the oil phase, a decrease in the surface active molecular weight on the oil–water interface, and an increase in IFT_{equ} [31]. In addition, enhanced hydrophobicity makes surfactant molecules more likely to associate to form micelles, and the number of single surfactant molecules at the oil–water interface decreases, while IFT_{equ} increases. This rule also applies to Ca^{2+} and Mg^{2+}.

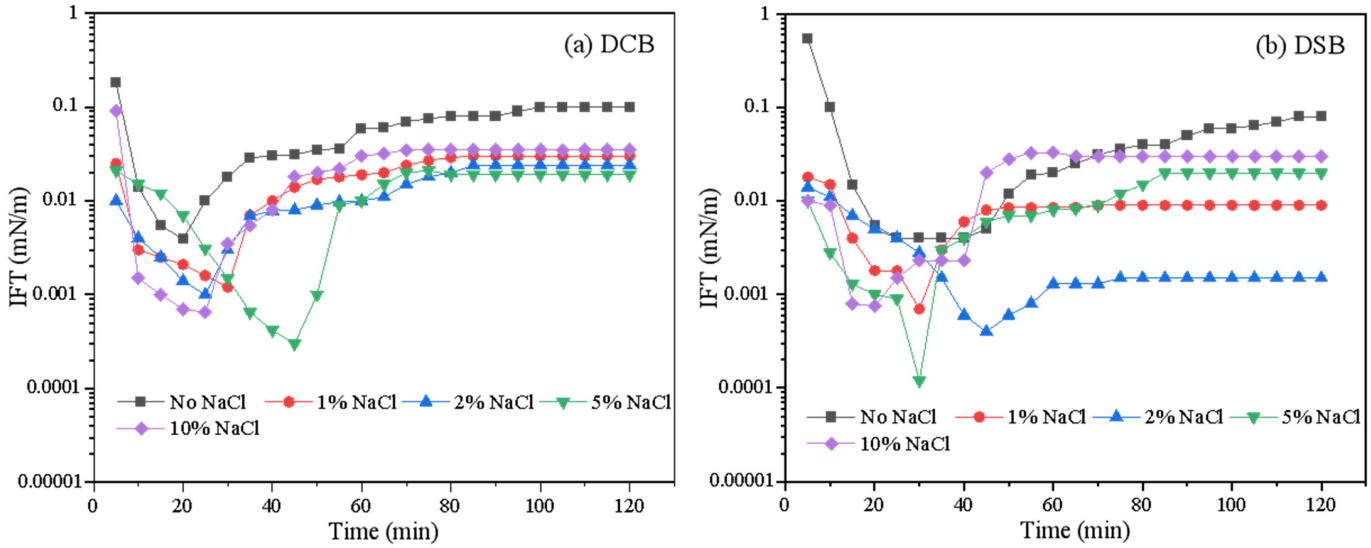

Figure 5. Effects of sodium chloride on IFT between the optimum concentrations of surfactants and Xinjiang crude oil at 40 °C for DCB (**a**) and DSB (**b**).

3.3.4. Effect of $CaCl_2$/$MgCl_2$ on IFT

Figure 6 shows the DIFT of DCB/DSB at different concentrations of $CaCl_2$/$MgCl_2$. It can be observed that the addition of Ca^{2+} and Mg^{2+} also showed a synergistic effect on the reduction in IFT. For DCB, when the concentration of Ca^{2+} ranges from 0.01% to 0.5%, the surfactant can reach an ultra-low interfacial tension level and the minimum value (7.9×10^{-4} mN/m) is reached when the concentration of Ca^{2+} is 0.2%. For DSB, when the Ca^{2+} concentration is 0.01–1%, the surfactant can reach an ultra-low interfacial tension level and a minimum value (7.2×10^{-4} mN/m) is reached.

The addition of Mg^{2+} has a more significant effect on IFT and also has a synergistic effect. For DCB, when the concentration of Mg^{2+} ranges from 0.01% to 0.2%, the surfactant can reach an ultra-low interfacial tension level and the minimum value (6.5×10^{-4} mN/m) is reached when the concentration of Mg^{2+} is 0.2%. For DSB, when the concentration of Mg^{2+} ranges from 0.01% to 0.2%, the surfactant can reach an ultra-low interfacial tension level and the minimum value (1.1×10^{-3} mN/m) is reached when the concentration of Mg^{2+} is 0.01%. Compared with Ca^{2+}, the surfactant showed lower tolerance to Mg^{2+}. The reason is that the bonding ability of Mg^{2+} is stronger than that of Ca^{2+} and more easily binds with surfactant ionic groups [32], and the molecular hydrophobicity is enhanced, which leads to a transfer from the oil–water interface to the oil phase under the condition of low solution concentration, resulting in the increase in IFT.

DSB has higher tolerance to divalent cations than DCB (Ca^{2+}: DCB tolerance range is 0.01–0.5%, DSB tolerance range is 0.01–1%; Mg^{2+}: DCB tolerance range is 0.01–0.2%, DSB tolerance range is 0.01–0.2%). Compared with the carboxyl group, the hydroxypropyl sulfonyl is a strong acid group, and the inner salt structure formed by the quaternary ammonium group in the molecule is more stable and not sensitive to the external electrolyte ions, so it has a higher tolerance. In conclusion, the effect of cations on IFT is as follows: $Na^+ < Ca^{2+} < Mg^{2+}$; it is thought that the binding degree between an ion head group and counterion increases with a rise in ionic polarizability and valence state and decreases with a rise in hydration radius.

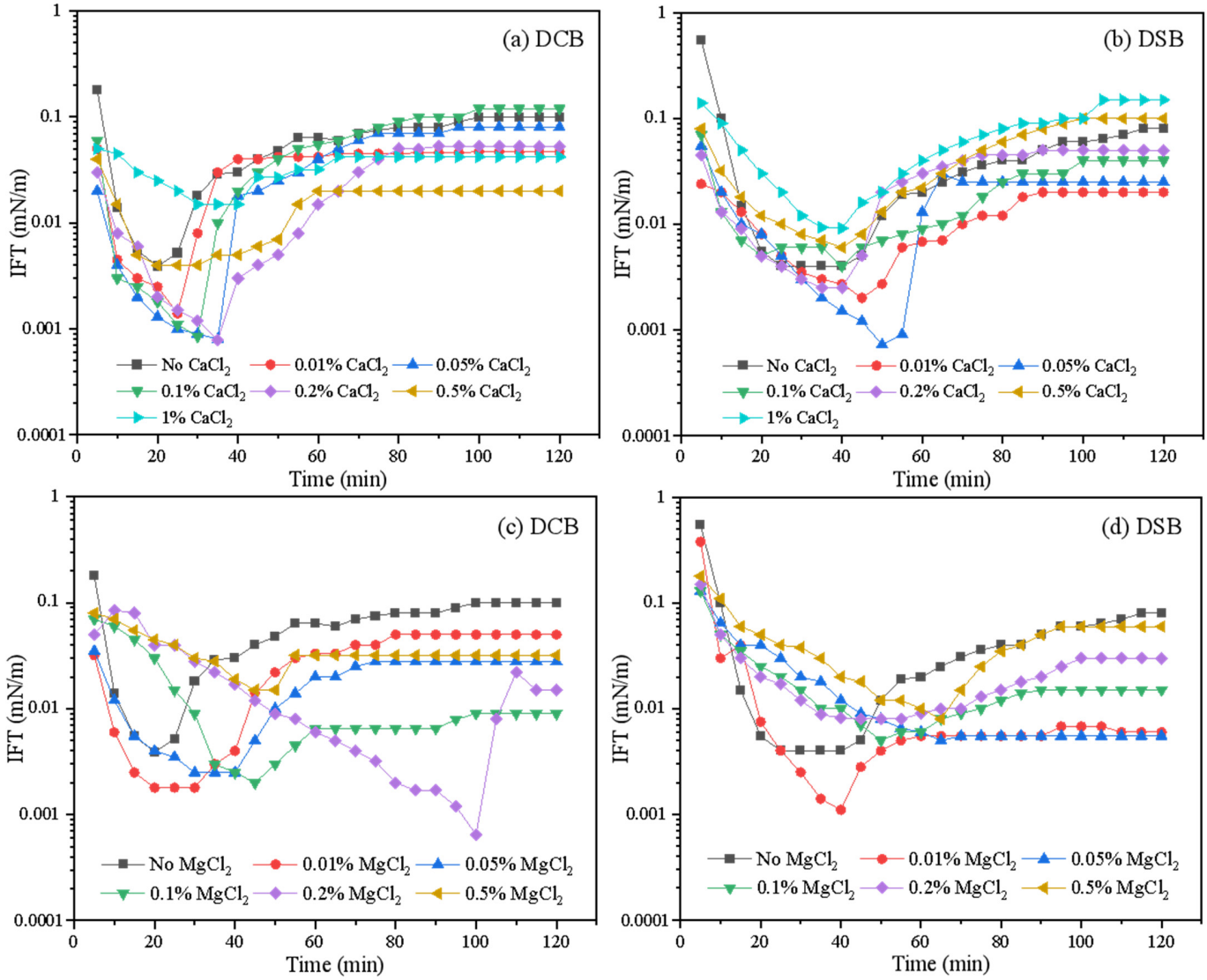

Figure 6. Effects of divalent ion on IFT between the optimum concentrations of surfactants and Xinjiang crude oil at 40 °C for DCB (**a**) and DSB (**b**) of $CaCl_2$, DCB (**c**) and DSB (**d**) of $MgCl_2$.

3.4. Wetting Ability

In tertiary oil recovery, an important mechanism of surfactant displacement is to change the wettability of formation rocks. In the process of displacement, surfactants with amphiphilic groups can be arranged at the interface between the rock and the liquid, so that the rock surface changes from the oleophilic surface to the hydrophilic surface. A change in wettability reduces the adhesion of oil droplets on the rock surface, and it is easier to be displaced by oil displacement agents [24,33].

With pure water as a blank control group, it was found that the droplet volume and contact angle did not change significantly over time, so the effect of water evaporation could be ignored. Figure 7 shows that the contact angle decreased sharply with the increase in surfactant concentration [19]. This is due to the concentration difference between the solution body and the solid–liquid interface continuing to increase, and the trend and probability of surfactant molecules diffusing to the interface increase, and the adsorption process becoming easier [34]. Meanwhile, ignoring the effect of water droplets evaporation at room temperature, the contact angle gradually tended toward stability, indicating that the adsorption of surfactant molecules on the interface is a dynamic process, and when the adsorption and desorption reached a dynamic equilibrium, the contact angle reached a stable value.

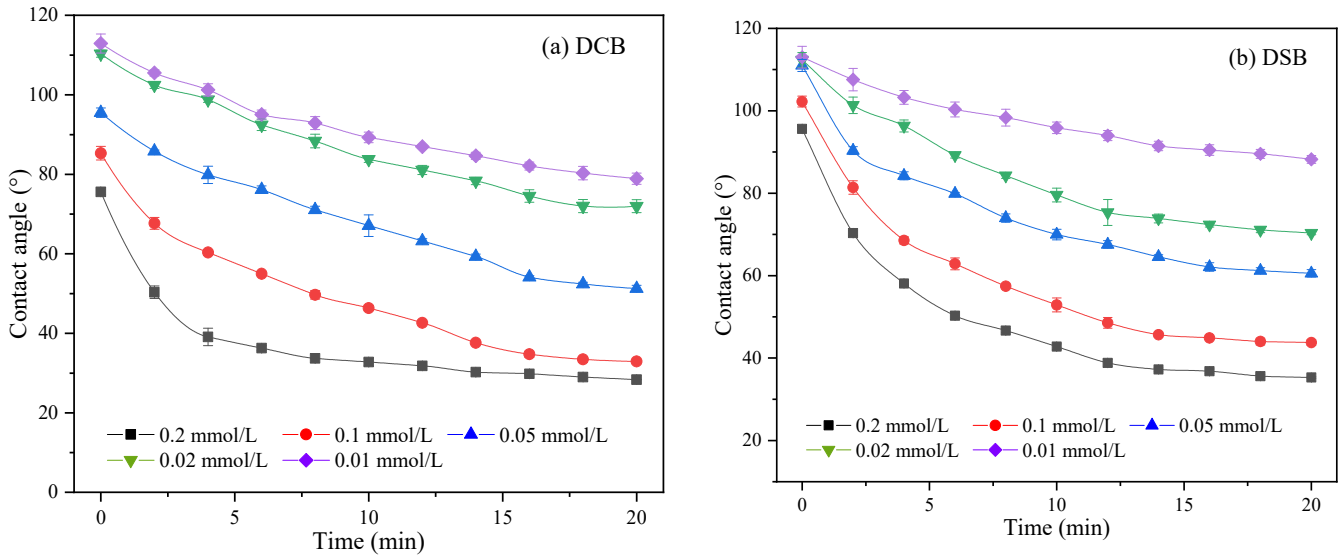

Figure 7. Variation of the contact angle with different surfactant concentrations on the paraffin surface at 25 °C for DCB (**a**) and DSB (**b**).

Figure 8 shows the dynamic contact angle changes of DCB and DSB using paraffin film as substrate. DCB and DSB showed the lowest contact angles of 28.36° and 35.26°, respectively, which can transform the oil-philic interface into a strong hydrophilic interface. DCB has a stronger wetting reversal ability and faster change rate of interface wettability, which can reduce the contact angle to less than 80° in a few seconds. This is because the carboxyl group volume is smaller than the hydroxypropyl sulfonic group, and the molecules are more tightly arranged and have stronger wettability when adsorbed on the interface [35].

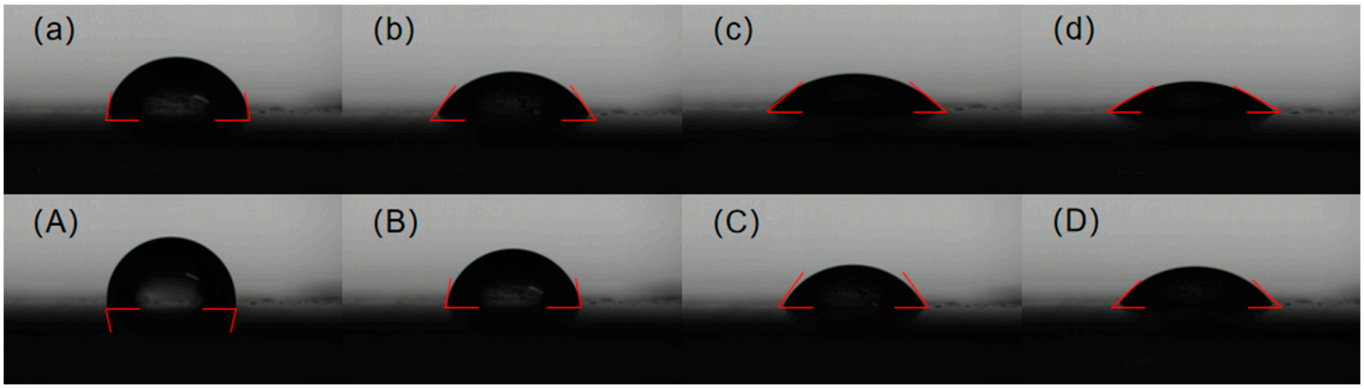

Figure 8. Contact angle images of 0.2 mmol/L DCB (**a**–**d**) and DSB (**A**–**D**) solutions on paraffin surface at different times: (**a**) 0 min, 75.60°; (**b**) 2 min, 50.33°; (**c**) 10 min, 32.78°; (**d**) 20 min, 28.36° for DCB and (**A**) 0 min, 95.60°; (**B**) 2 min, 70.33°; (**C**) 10 min, 42.78°; (**D**) 20 min, 35.26° for DSB.

3.5. Emulsion Stability

The principle of emulsifying performance is to emulsify crude oil into an O/W emulsion and displace crude oil from rock fractures, which is used as an important reference standard for the application of surfactants in oilfields. The adsorption of surfactants at the interface reduces the interfacial free energy, forming a layer with a different composition and a much higher solute concentration than the inner part of the solution. The interfacial layer formed by substance enrichment determines the stability of the emulsion.

The Table 2 shows that, with the increase in temperature, the water separation time of the emulsion is shortened and the emulsifying property weakened. With the increase in

temperature, the viscosity of the system decreases and the touching rate of water droplets increases, which leads to a decrease in system stability and the shortening of demulsification time. It can also be observed that, with the increase in surfactant solution concentration, the water separation time of the emulsion showed a trend of first increasing and then decreasing. When the concentration was 0.2 g/L, DCB and DSB took the longest time to separate 10 mL water: 401 s and 428 s, respectively. When the solution concentration was low, the molecules were loosely arranged in the interfacial film and the emulsion formed was unstable. With the increase in concentration, the molecules were closely arranged at the interface and the strength of the interface film was high, which hindered the aggregation of liquid beads and increased the stability of the emulsion. However, as the surfactant concentration continued to increase, the solution tended to be saturated, and the excess surfactant molecules aggregated with each other, resulting in the flocculation of the oil phase dispersed in the system, and the demulsification time became shorter.

Table 2. Emulsification time of DCB and DSB at different concentrations and temperatures.

		0.05 g/L	0.1 g/L	0.15 g/L	0.2 g/L	0.25 g/L	0.3 g/L
DCB emulsion stability time/s	25 °C	212	351	364	401	382	375
	45 °C	208	277	319	340	336	301
	75 °C	186	224	232	258	245	220
DSB emulsion stability time/s	25 °C	233	37	392	428	428	418
	45 °C	223	341	350	371	365	330
	75 °C	201	249	253	269	250	225

4. Conclusions

In this study, two new betaine surfactants (DCB and DSB) were prepared for the first time, and their chemical structures were characterized using ^{1}H-NMR and ^{13}C-NMR. The sulfobetaine exhibited higher thermal stability than the carboxyl betaine, and the initial thermal decomposition temperatures of DSB and DCB were 240 °C and 193 °C, respectively. DCB showed lower surface tension, mainly because the volume of the carboxyl group was smaller than that of the hydroxypropyl sulfonic group, and the arrangement of betaine molecules was closer after saturation adsorption on the liquid surface. In addition, the lower CMC of DSB is the result of solvation, because during micelle formation, the hydroxypropyl sulfonic group and the carboxyl group may have different solvation/desolvation characteristics. The interfacial tension measurements indicated that DSB had higher tolerance to divalent cations than DCB (Ca^{2+}: DCB tolerance range was 0.01–0.5% and DSB tolerance range was 0.01–1%; Mg^{2+}: DCB tolerance range was 0.01–0.2% and DSB tolerance range was 0.01–0.2%). In terms of reducing IFT, Na^{+}, Ca^{2+}, and Mg^{2+} showed similar synergistic effects with betaine surfactant molecules. DCB and DSB solutions completely moistened the paraffin film according to the measurements of wetting ability and the lowest contact angles were 28.36° and 35.26°, respectively. In conclusion, these two kinds of betaine surfactants have the potential to be used in high-temperature and -salt reservoirs.

Supplementary Materials: The following supporting information can be downloaded at https://www.mdpi.com/article/10.3390/app13074378/s1, Figure S1: ^{1}H NMR spectra of 1-chloro-3-(4-dodecylphenoxy)propan-2-ol in $CDCl_3$; Figure S2: ^{13}C NMR spectra of 1-chloro-3-(4-dodecylphenoxy)propan-2-ol in $CDCl_3$; Figure S3: ^{1}H NMR spectra of 1-((3-(4-dodecylphenoxy)-2-hydroxypropyl)-dimethylammonio)acetate in CD_3OD; Figure S4: ^{13}C NMR spectra of 1-((3-(4-dodecylphenoxy)-2-hydroxypropyl)-dimethylammonio)acetate in CD_3OD; Figure S5: ^{1}H NMR spectra of 1-((3-(4-dodecylphenoxy)-2-hydroxypropyl)-dimethylammonio)-2-hydroxypropane-1-sulfonate in CD_3OD. Figure S6: ^{13}C NMR spectra of 1-((3-(4-dodecylphenoxy)-2-hydroxypropyl) -dimethylammonio)-2-hydroxypropane-1-sulfonate in CD_3OD.

Author Contributions: Conceptualization, Q.Z. and Z.W.; methodology, Q.Z.; software, L.Y.; validation, Q.Z., Z.W. and P.L.; formal analysis, Z.W. and P.L.; investigation, Q.Z. and Z.W.; resources, Z.S.; data curation, L.Y.; writing—original draft preparation, Q.Z.; writing—review and editing, Q.Z., Z.W. and P.L.; visualization, P.L.; supervision, L.Y.; project administration, Q.Z. and Z.S.; funding acquisition, Z.S. All authors have read and agreed to the published version of the manuscript.

Funding: This research was funded by the State Key Laboratory of Shale Oil and Gas Enrichment Mechanisms and Effective Development (No: 33550000-22-ZC0613-0028).

Institutional Review Board Statement: Not applicable.

Informed Consent Statement: Not applicable.

Data Availability Statement: The data used to support the findings of this study are included within the article.

Conflicts of Interest: The authors declare no conflict of interest.

References

1. Kelleppan, V.T.; King, J.P.; Butler, C.S.G.; Williams, A.P.; Tuck, K.L.; Tabor, R.F. Heads or tails? The synthesis, self-assembly, properties and uses of betaine and betaine-like surfactants. *Adv. Colloid Interface Sci.* **2021**, *297*, 102528. [CrossRef]
2. Shakil Hussain, S.M.; Kamal, M.S.; Fogang, L.T. Effect of internal olefin on the properties of betaine-type zwitterionic surfactants for enhanced oil recovery. *J. Mol. Liq.* **2018**, *266*, 43–50. [CrossRef]
3. Eastoe, J.; Tabor, R.F. Chapter 6-Surfactants and Nanoscience. In *Colloidal Foundations of Nanoscience*; Berti, D., Palazzo, G., Eds.; Elsevier: Amsterdam, The Netherlands, 2014; pp. 135–157. [CrossRef]
4. Singh, K.; Marangoni, D.G. Synergistic interactions in the mixed micelles of cationic gemini with zwitterionic surfactants: The pH and spacer effect. *J. Colloid Interface Sci.* **2007**, *315*, 620–626. [CrossRef] [PubMed]
5. Wu, A.; Gao, Y.; Zheng, L. Zwitterionic amphiphiles: Their aggregation behavior and applications. *Green Chem.* **2019**, *21*, 4290–4312. [CrossRef]
6. Chen, S.; Liu, H.; Sun, H.; Yan, X.; Wang, G.; Zhou, Y.; Zhang, J. Synthesis and physiochemical performance evaluation of novel sulphobetaine zwitterionic surfactants from lignin for enhanced oil recovery. *J. Mol. Liq.* **2018**, *249*, 73–82. [CrossRef]
7. Uphues, G. Chemistry of amphoteric surfactants. *Fett-Lipid* **1998**, *100*, 490–497. [CrossRef]
8. Demirbas, A.; Alsulami, H.E.; Hassanein, W.S. Utilization of Surfactant Flooding Processes for Enhanced Oil Recovery (EOR). *Pet. Sci. Technol.* **2015**, *33*, 1331–1339. [CrossRef]
9. Hu, X.; Qi, D.; Yan, L.; Cui, Z.; Song, B.; Pei, X.; Jiang, J. Inhibiting hydrophobization of sandstones via adsorption of alkyl carboxyl betaines in SP flooding by using gentle alkali. *Colloids Surf. A Physicochem. Eng. Asp.* **2017**, *535*, 75–82. [CrossRef]
10. Chen, Z.; Li, Y.-L.; Liu, X.; Cui, Z. Dialkyl Sulfobetaine Surfactants Derived from Guerbet Alcohol Polyoxypropylene–Polyoxyethylene Ethers for SP Flooding of High Temperature and High Salinity Reservoirs. *J. Surfactants Deterg.* **2021**, *24*, 421–432. [CrossRef]
11. Wang, Y.; Liu, J.; Liu, B.-J.; Liu, Y.; Wang, H.; Chen, G. Why Does Scale Form in ASP Flood? How to Prevent from It? A Case Study of the Technology and Application of Scaling Mechanism and Inhibition in ASP Flood Pilot Area of N-1DX Block in Daqing. In Proceedings of the 6th International Symposium on Olfield Scale, Aberdeen, UK, 26–27 May 2004.
12. Guo, H.; Yiqiang, L.; Yanyue, L.; Kong, D.; Li, B.; Wang, F. Lessons Learned from ASP Flooding Tests in China. In Proceedings of the SPE Reservoir Characterisation and Simulation Conference, Abu Dhabi, United Arab Emirates, 8–10 May 2017.
13. Zhao, Z.; Liu, F.; Qiao, W.; Li, Z.; Cheng, L. Novel alkyl methylnaphthalene sulfonate surfactants: A good candidate for enhanced oil recovery. *Fuel* **2006**, *85*, 1815–1820. [CrossRef]
14. Li, P.; Yang, C.; Cui, Z.; Song, B.; Jiang, J.; Wang, Z. A New Type of Sulfobetaine Surfactant with Double Alkyl Polyoxyethylene Ether Chains for Enhanced Oil Recovery. *J. Surfactants Deterg.* **2016**, *19*, 967–977. [CrossRef]
15. Dong, L.; Cao, X.; Li, Z.; Zhang, L.; Xu, Z.; Zhang, L.; Zhao, S. Dilational rheological properties of novel zwitterionic surfactants containing benzene ring and polyoxyethylene group at water–decane interface. *Colloids Surf. A Physicochem. Eng. Asp.* **2014**, *444*, 257–268. [CrossRef]
16. Zhou, Z.-H.; Zhang, Q.; Liu, Y.; Wang, H.-Z.; Cai, H.-Y.; Zhang, F.; Tian, M.-Z.; Liu, Z.-Y.; Zhang, L.; Zhang, L. Effect of Fatty Acids on Interfacial Tensions of Novel Sulfobetaines Solutions. *Energy Fuels* **2014**, *28*, 1020–1027. [CrossRef]
17. Gao, S.; Song, Z.; Lan, F.; Zhao, J.; Xu, T.; Du, Y.; Jiang, Q. Synthesis and Physicochemical Properties of Novel Phenyl-Containing Sulfobetaine Surfactants. *Ind. Eng. Chem. Res.* **2019**, *58*, 15479–15488. [CrossRef]
18. Gao, S.; Song, Z.; Zhu, D.; Lan, F.; Jiang, Q. Synthesis, surface activities, and aggregation behavior of phenyl-containing carboxybetaine surfactants. *RSC Adv.* **2018**, *8*, 33256–33268. [CrossRef] [PubMed]
19. Kumar, A.; Mandal, A. Synthesis and physiochemical characterization of zwitterionic surfactant for application in enhanced oil recovery. *J. Mol. Liq.* **2017**, *243*, 61–71. [CrossRef]
20. Kamal, M.S.; Hussein, I.A.; Sultan, A.S. Review on Surfactant Flooding: Phase Behavior, Retention, IFT, and Field Applications. *Energy Fuels* **2017**, *31*, 7701–7720. [CrossRef]

21. Shen, J.; Bai, Y.; Tai, X.; Wang, W.; Wang, G. Surface Activity, Spreading, and Aggregation Behavior of Ecofriendly Perfluoropolyether Amide Propyl Betaine in Aqueous Solution. *ACS Sustain. Chem. Eng.* **2018**, *6*, 6183–6191. [CrossRef]
22. Sreenu, M.; Prasad, R.B.N.; Sujitha, P.; Kumar, C.G. Synthesis and Surface-Active Properties of Sodium *N*-Acylphenylalanines and Their Cytotoxicity. *Ind. Eng. Chem. Res.* **2015**, *54*, 2090–2098. [CrossRef]
23. Qiao, M.; Zhao, N.; Zhao, Y.; Wu, W.; Zhang, X.; Li, X.; Dong, Y. Synthesis and effect of double-anion surfactant for oil displacement. *Oilfield Chem.* **2017**, *34*, 113–118. [CrossRef]
24. Hu, S.-S.; Zhang, L.; Xu, Z.-C.; Gong, Q.-T.; Jin, Z.-Q.; Luo, L.; Zhang, L.; Zhao, S. Wettability alteration by novel betaines at polymer–aqueous solution interfaces. *Appl. Surf. Sci.* **2015**, *355*, 868–877. [CrossRef]
25. Gerola, A.P.; Costa, P.F.A.; Nome, F.; Quina, F. Micellization and adsorption of zwitterionic surfactants at the air/water interface. *Curr. Opin. Colloid Interface Sci.* **2017**, *32*, 48–56. [CrossRef]
26. Qiao, W.; Cui, Y.; Zhu, Y.; Cai, H. Dynamic interfacial tension behaviors between Guerbet betaine surfactants solution and Daqing crude oil. *Fuel* **2012**, *102*, 746–750. [CrossRef]
27. Qiao, W.; Li, J.; Zhu, Y.; Cai, H. Interfacial tension behavior of double long-chain 1,3,5-triazine surfactants for enhanced oil recovery. *Fuel* **2012**, *96*, 220–225. [CrossRef]
28. Zhong, Q.-L.; Zhou, Z.-H.; Zhang, Q.; Ma, D.-S.; Luan, H.-X.; Zhang, L.; Ma, G.-Y.; Zhang, L. Studies on Interfacial Tensions of Ionic Surfactant and Alkyl Sulfobetaine Mixed Solutions. *Energy Fuels* **2018**, *32*, 8202–8209. [CrossRef]
29. Aoudia, M.; Al-Shibli, M.N.; Al-Kasimi, L.H.; Al-Maamari, R.; Al-bemani, A. Novel surfactants for ultralow interfacial tension in a wide range of surfactant concentration and temperature. *J. Surfactants Deterg.* **2006**, *9*, 287–293. [CrossRef]
30. Bera, A.; Mandal, A.; Guha, B. Synergistic Effect of Surfactant and Salt Mixture on Interfacial Tension Reduction between Crude Oil and Water in Enhanced Oil Recovery. *J. Chem. Eng. Data* **2014**, *59*, 89–96. [CrossRef]
31. Zhang, Q.-Q.; Cai, B.-X.; Xu, W.-J.; Gang, H.-Z.; Liu, J.-F.; Yang, S.-Z.; Mu, B.-Z. Novel zwitterionic surfactant derived from castor oil and its performance evaluation for oil recovery. *Colloids Surf. A Physicochem. Eng. Asp.* **2015**, *483*, 87–95. [CrossRef]
32. Liu, Z.; Zhang, L.; Cao, X.; Song, X.; Jin, Z.; Zhang, L.; Zhao, S. Effect of Electrolytes on Interfacial Tensions of Alkyl Ether Carboxylate Solutions. *Energy Fuels* **2013**, *27*, 3122–3129. [CrossRef]
33. Kumar, A.; Mandal, A. Characterization of rock-fluid and fluid-fluid interactions in presence of a family of synthesized zwitterionic surfactants for application in enhanced oil recovery. *Colloids Surf. A Physicochem. Eng. Asp.* **2018**, *549*, 1–12. [CrossRef]
34. Niu, R.; He, J.; Long, B.; Wang, D.; Song, H.; Wang, C.; Qu, G. Adsorption, wetting, foaming, and emulsification properties of mixtures of nonylphenol dodecyl sulfonate based on linear alpha-olefin and heavy alkyl benzene sulfonate. *J. Dispers. Sci. Technol.* **2017**, *39*, 1108–1114. [CrossRef]
35. Zhenggang, C.; Dan, Q.; Binglei, S.; Xiaomei, P.; Xin, H. Inhibiting Hydrophobization of Sandstones via Adsorption of Alkyl Carboxyl Betaines in Surfactant–Polymer Flooding Using Poly Alkylammonium Bromides. *Energy Fuels* **2016**, *30*, 2043–2051. [CrossRef]